Supporting Information

Facile Preparation of Novel and Active 2D Nanosheets from Non-layered and Traditionally Un-exfoliatable Earth-abundant Materials

Sheng Liu,†[1,2] Lei Xie,†[2] Hui Qian,[3] Guangyi Liu,[1] Hong Zhong,[1] and Hongbo Zeng*[2]*

[1]College of Chemistry and Chemical engineering, Central South University, Changsha, 410083, China

[2]Department of Chemical and Materials Engineering, University of Alberta, Edmonton, Alberta, T6G 1H9, Canada

[3]Nanotechnology Research Center, National Research Council, Edmonton, Alberta T6G 2M9, Canada

†Sheng Liu and Lei Xie contributed equally to this work.

**Email: hongbo.zeng@ualberta.ca (H. Zeng), Phone: +1-780-492-1044, Fax: +1-780-492-2881*

**Email: guangyiliu@csu.edu.cn (G. Liu)*

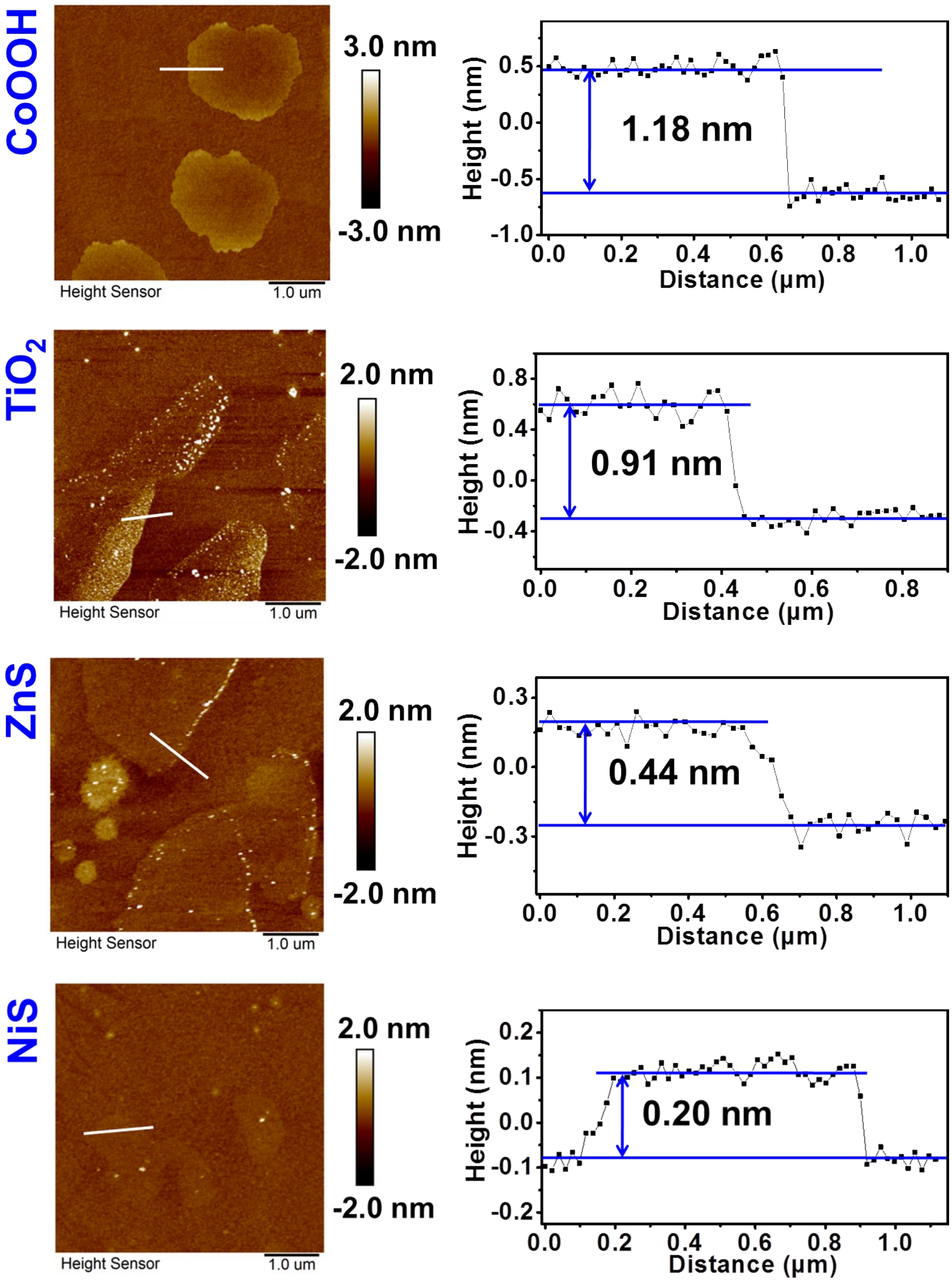
CoOOH
3.0 nm
-3.0 nm
Height Sensor
1.0 um
Height (nm)
Distance (μm)
1.18 nm
TiO2
2.0 nm
-2.0 nm
Height Sensor
1.0 um
Height (nm)
Distance (μm)
0.91 nm
ZnS
2.0 nm
-2.0 nm
Height Sensor
1.0 um
Height (nm)
Distance (μm)
0.44 nm
NiS
2.0 nm
-2.0 nm
Height Sensor
1.0 um
Height (nm)
Distance (μm)
0.20 nm

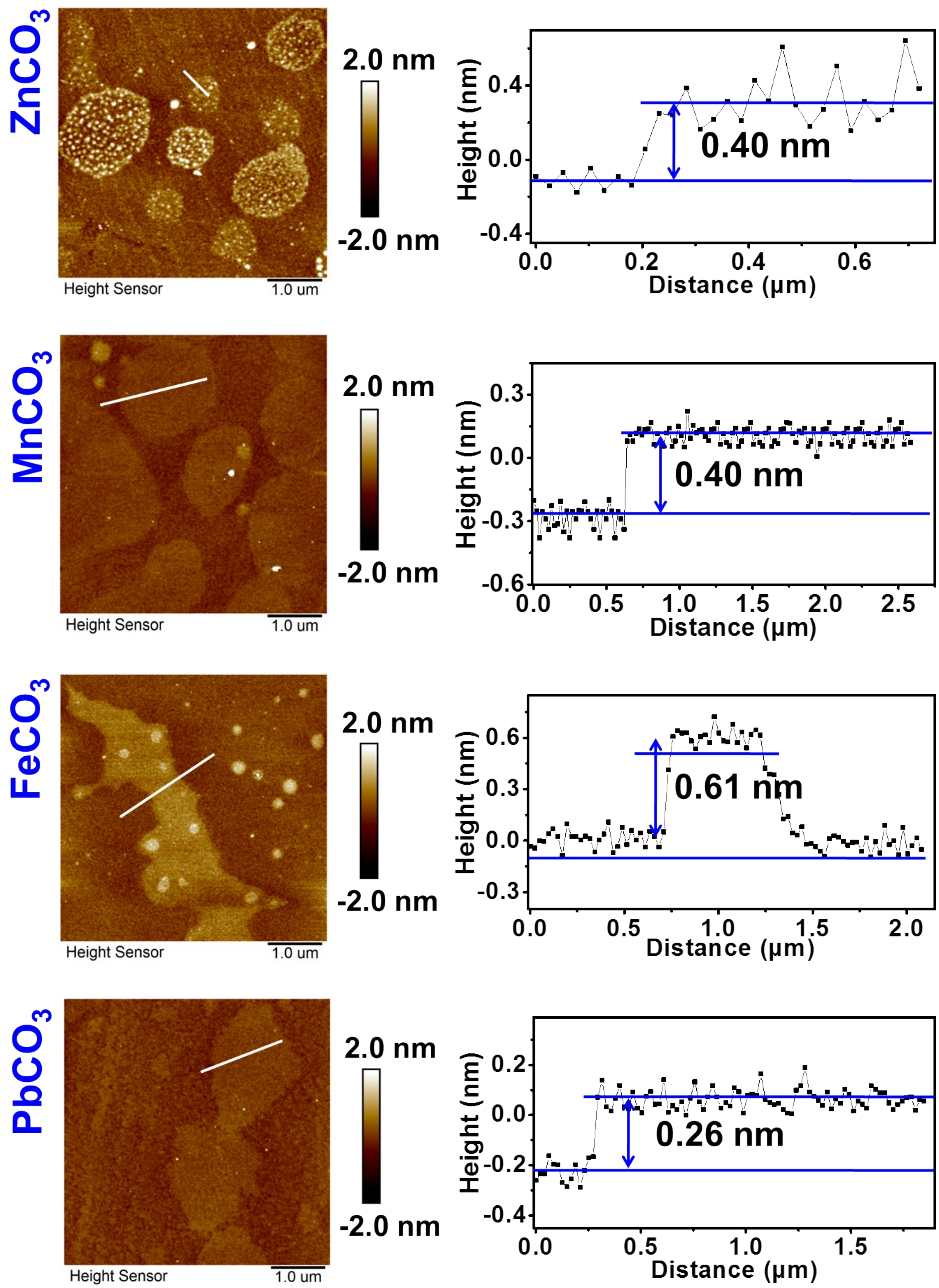
ZnCO3
2.0 nm
-2.0 nm
Height Sensor
1.0 um
0.40 nm
Height (nm)
Distance (μm)
MnCO3
2.0 nm
-2.0 nm
Height Sensor
1.0 um
0.40 nm
Height (nm)
Distance (μm)
FeCO3
2.0 nm
-2.0 nm
Height Sensor
1.0 um
0.61 nm
Height (nm)
Distance (μm)
PbCO3
2.0 nm
-2.0 nm
Height Sensor
1.0 um
0.26 nm
Height (nm)
Distance (μm)

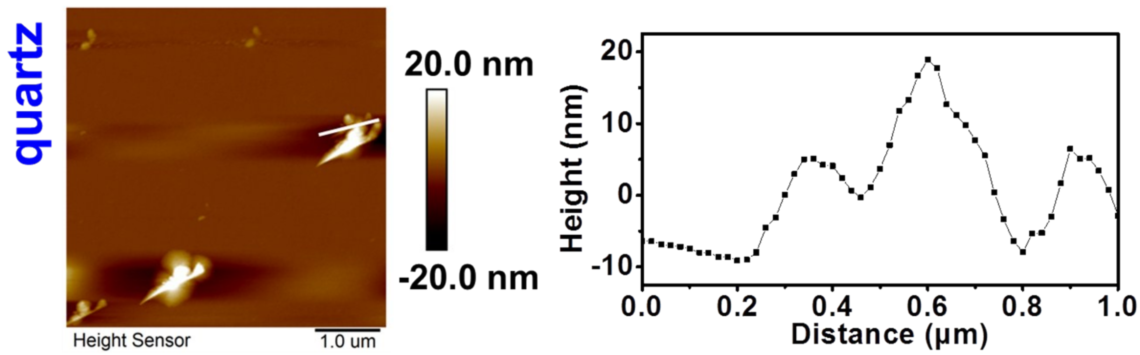

Figure S1. AFM topographic images (5×5 μm^2) and height profiles of the nanosheets exfoliated from non-layered oxides: CoOOH and TiO_2, sulfides: ZnS and NiS, and carbonates: $ZnCO_3$, $MnCO_3$, $FeCO_3$ and $PbCO_3$, with cleavage planes. Quartz without any cleavage plane as the control experiment only shows irregular small particles.

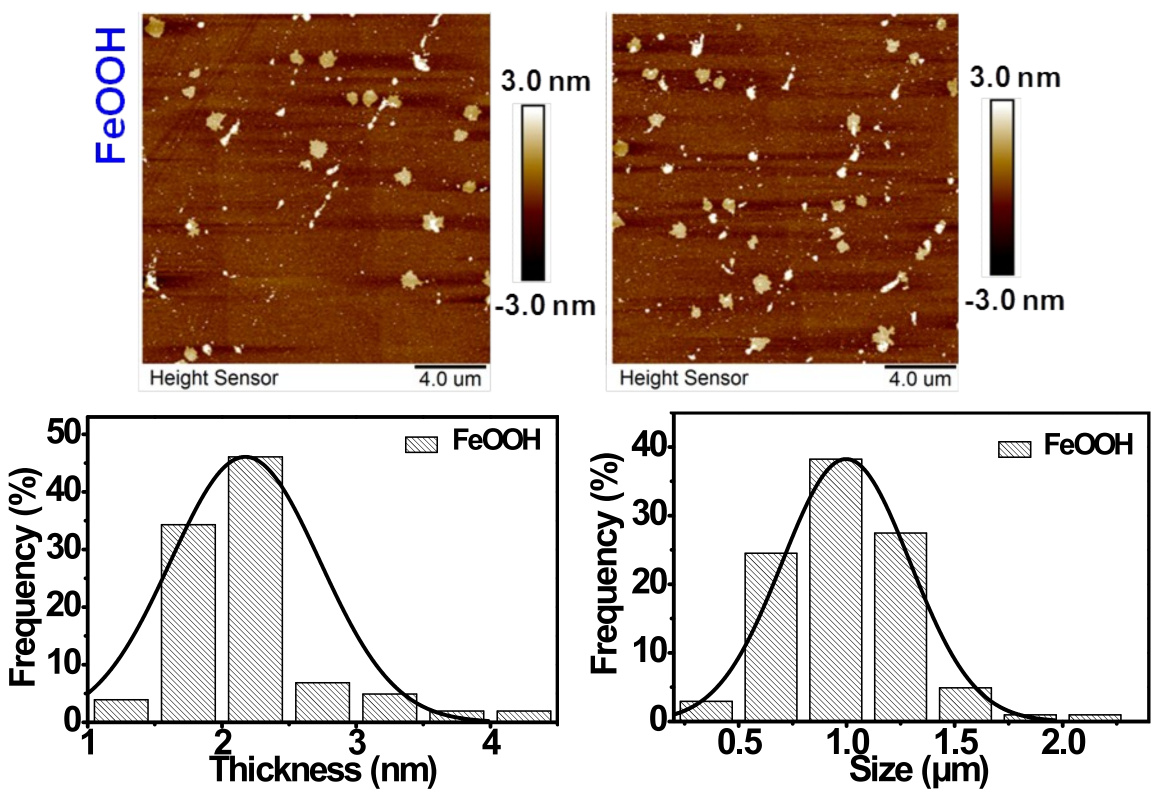

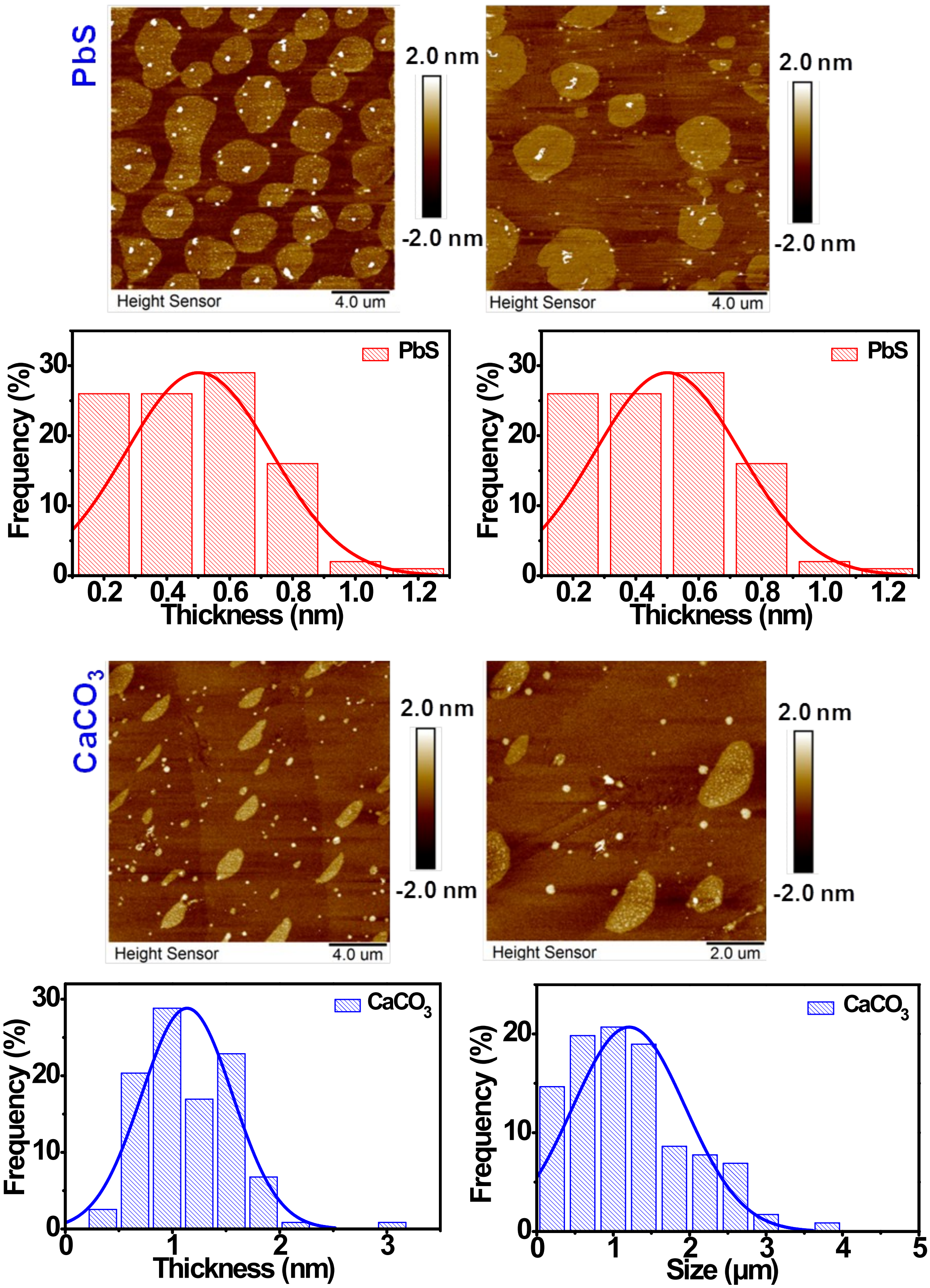

Figure S2. Typical AFM topographic images and distributions of thickness and size of α-FeOOH, PbS and $CaCO_3$ nanosheets.

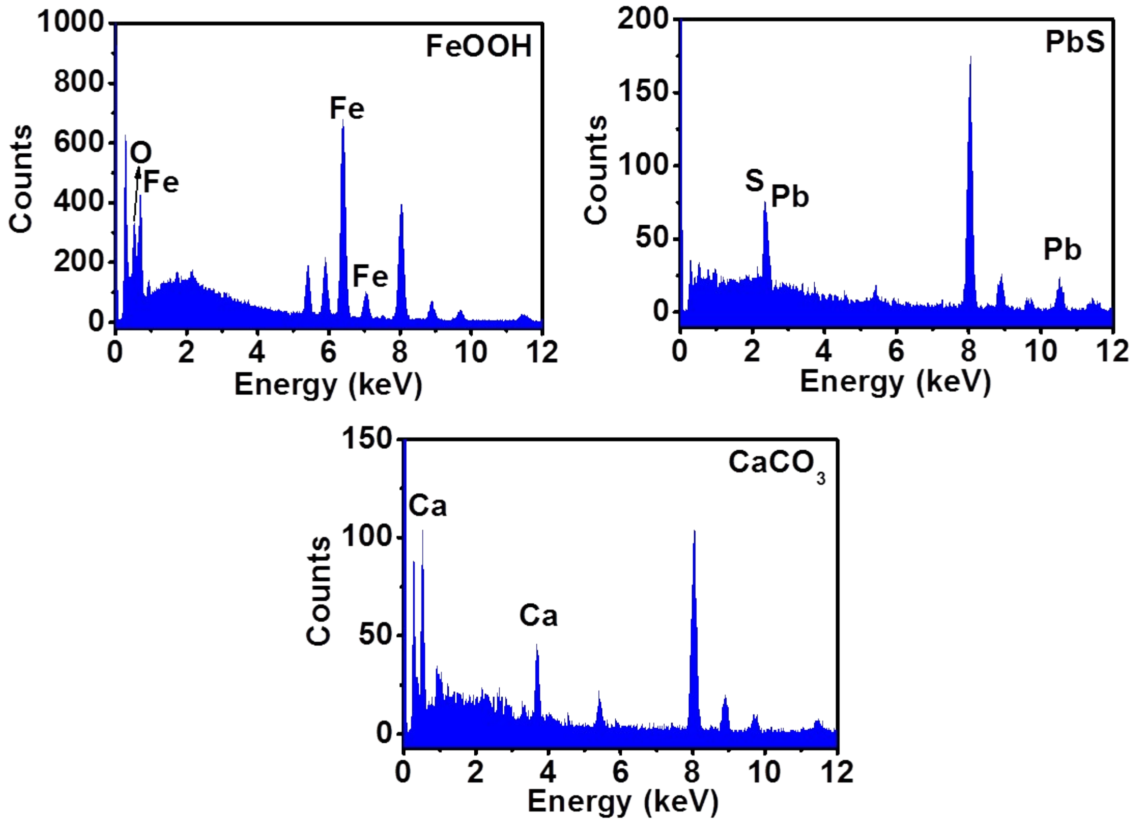

Figure S3. STEM-EDX analysis of α-FeOOH, PbS and $CaCO_3$ nanosheets. STEM-EXD confirms the chemical composition of exfoliated nanosheets for TEM characterization to be α-FeOOH, PbS and $CaCO_3$, respectively, and the contamination originated from the Cu source of TEM grids is inevitable.

Table S1. Atomic concentration obtained from STEM-EDX analysis.

Samples	Atomic concentration (%)					
	Fe	O	Pb	S	Ca	C
2D FeOOH	31.5	68.5				
2D PbS			48.3	51.7		
2D $CaCO_3$		59.1			17.1	23.8

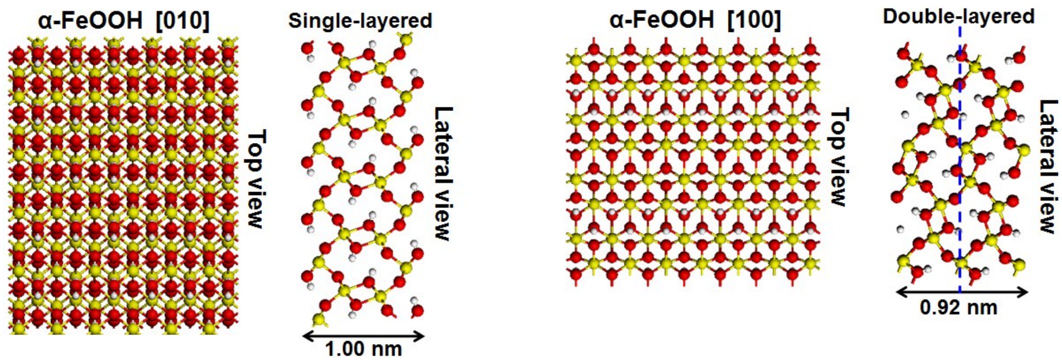

Figure S4. Atomic structures of α-FeOOH (010) and (100) cleavage planes.

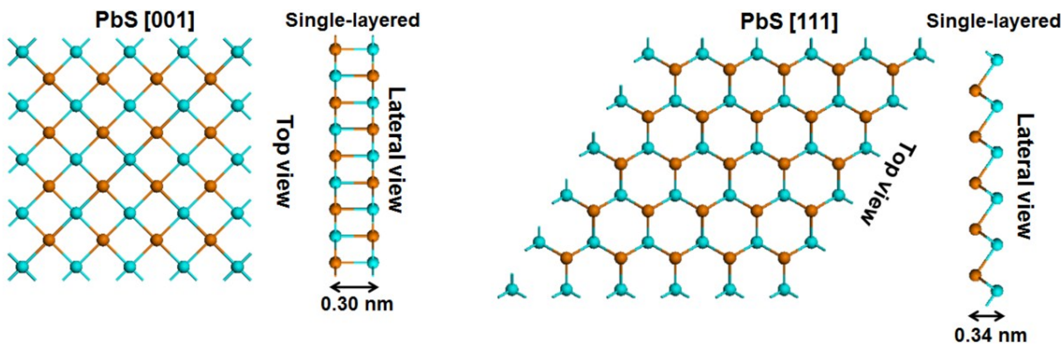

Figure S5. Atomic structures of PbS (001) and (111) cleavage planes.

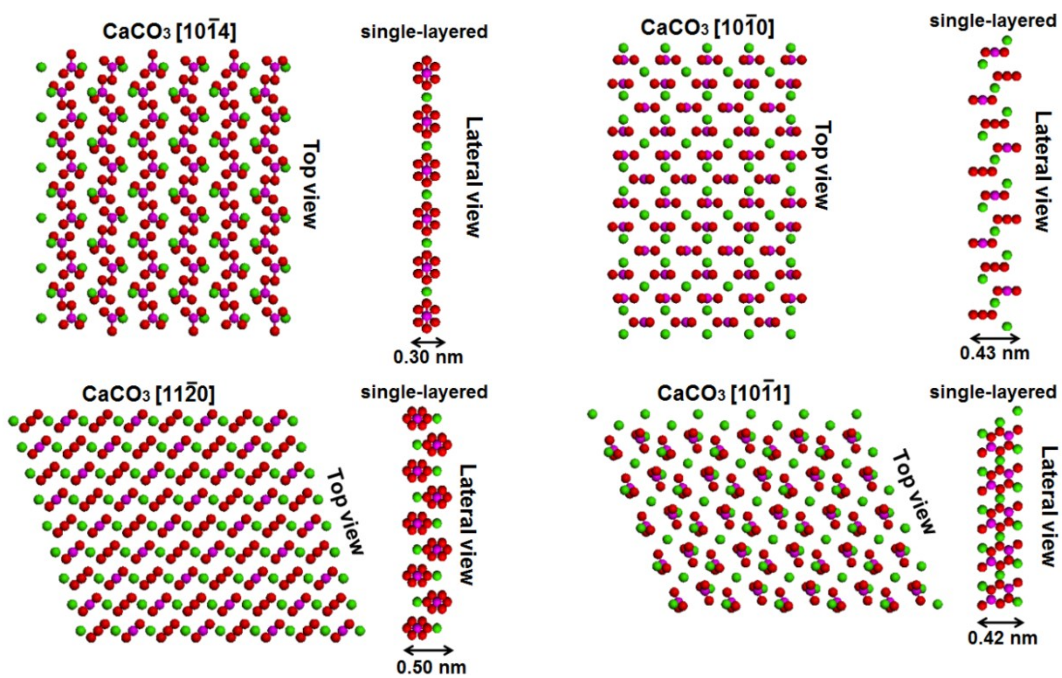

Figure S6. Atomic structures of $CaCO_3$ (10$\bar{1}$4), (10$\bar{1}$0), (11$\bar{2}$0) and (10$\bar{1}$1) cleavage planes.

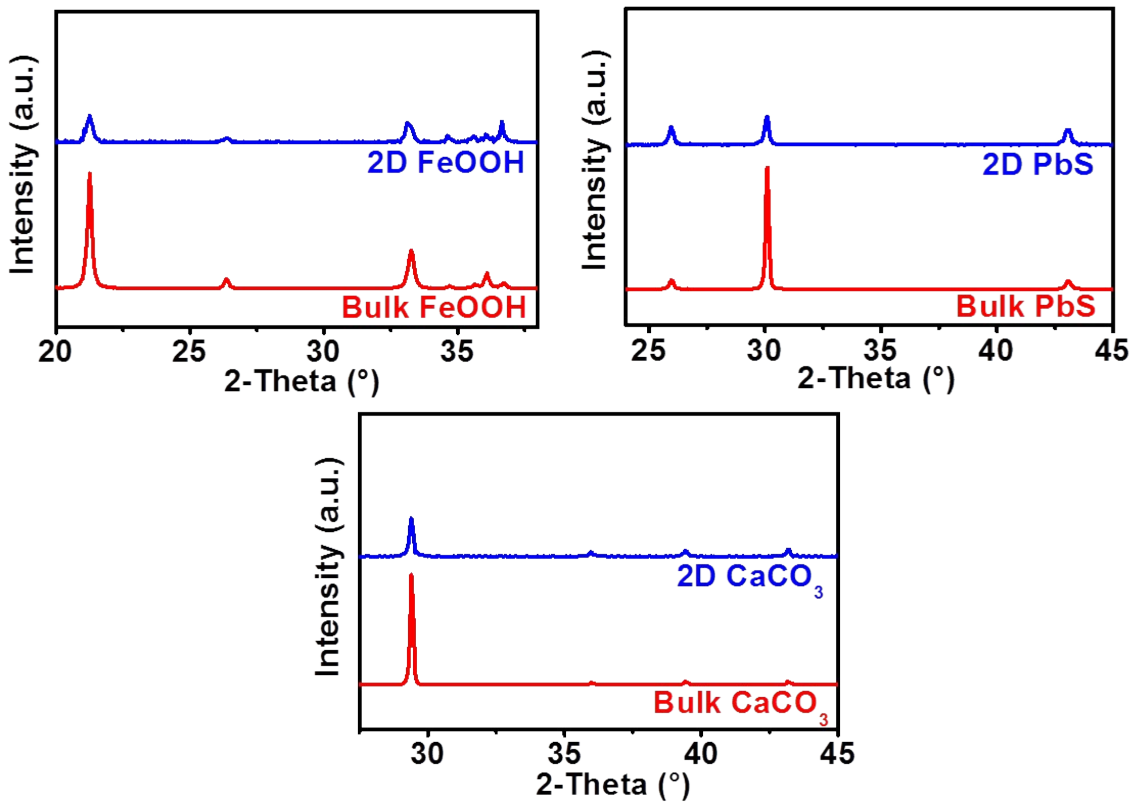

Figure S7. XRD of α-FeOOH, PbS and $CaCO_3$ nanosheets and pristine powders. The zoomed-in figures clearly show the stronger and broadened peaks for 2D nanosheets.

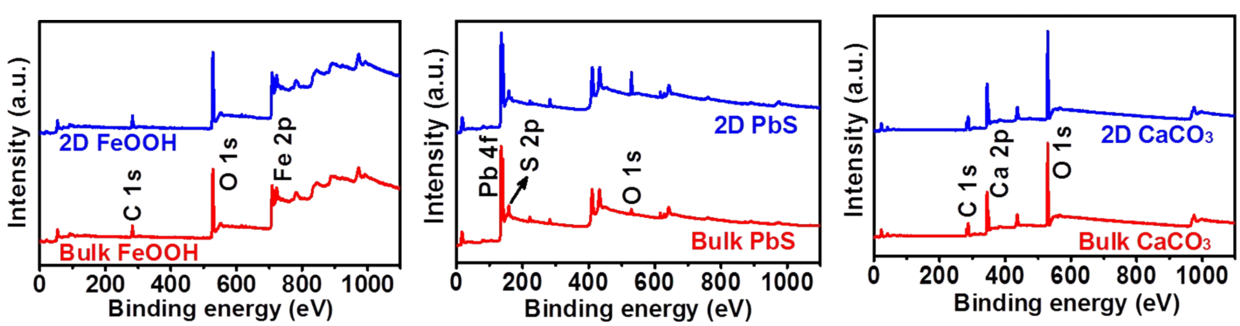

Figure S8. Survey scan XPS spectra of the exfoliated nanosheets and pristine powders of α-FeOOH, PbS and $CaCO_3$. Survey scan spectra confirm the purity of the exfoliated nanosheets and pristine powders since no impurity element was detected except the inevitable contamination of carbon and oxygen.

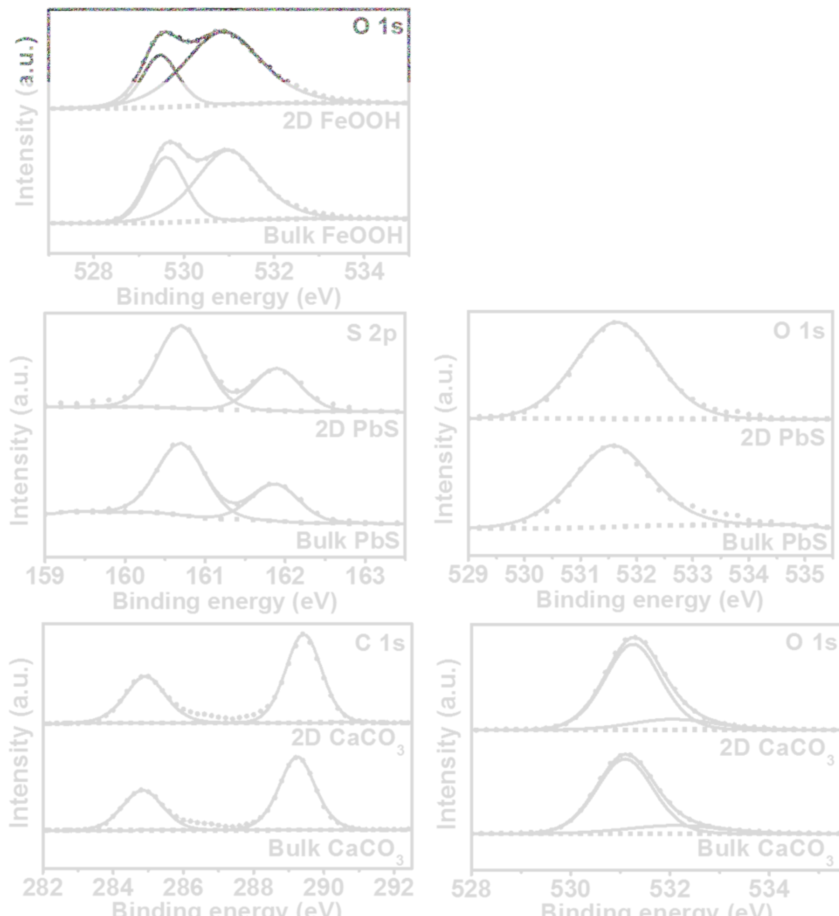

Figure S9. High-resolution XPS spectra of the exfoliated nanosheets and pristine powders of α-FeOOH, PbS and $CaCO_3$. It is noted that Fe 2p of α-FeOOH, Pb 4f of PbS and Ca 2p of $CaCO_3$ are shown in Figure 3. High-resolution spectra show the pristine chemical state with no obvious variation for both 2D α-FeOOH and 2D $CaCO_3$ while increased surface oxidation for 2D PbS.

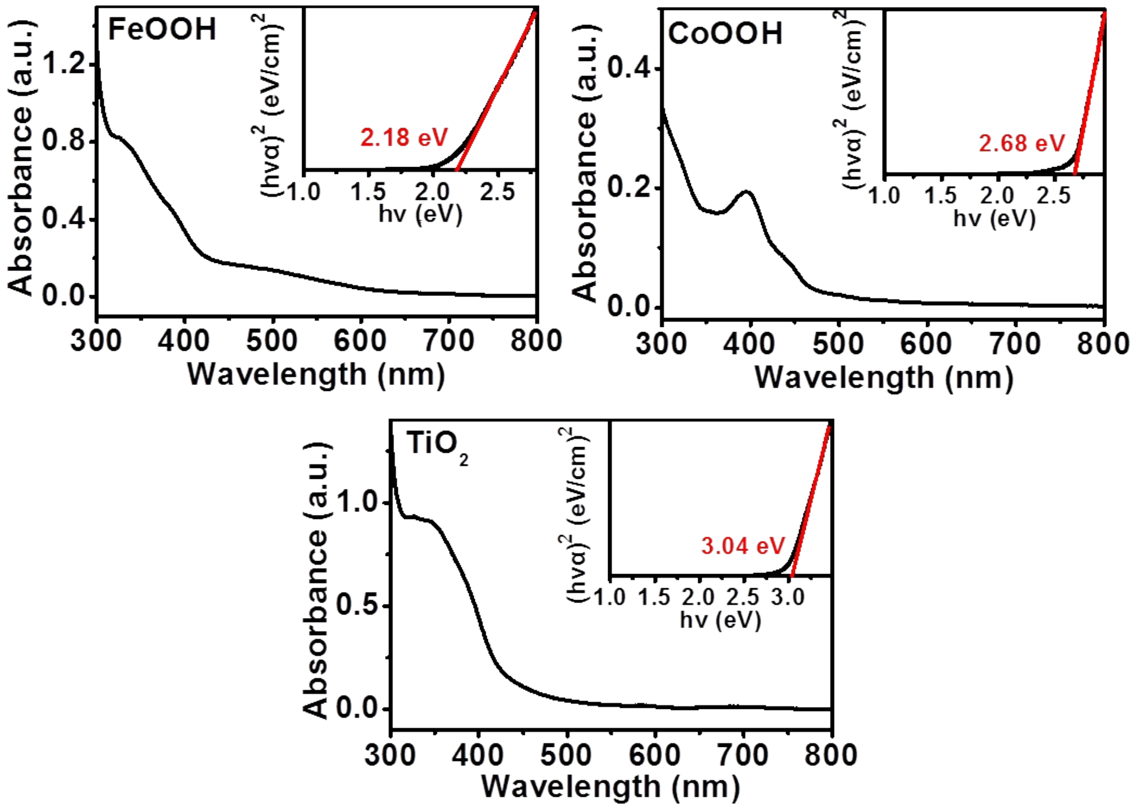

Figure S10. UV-vis absorption of α-FeOOH, CoOOH and TiO_2 nanosheets in DMF with the calculated optical band gap (inset). In general, the materials with reduced size and dimension display raised conduction band and lowered valence band, thereby resulting in a blueshift of the absorption edge and increase in the band gap.

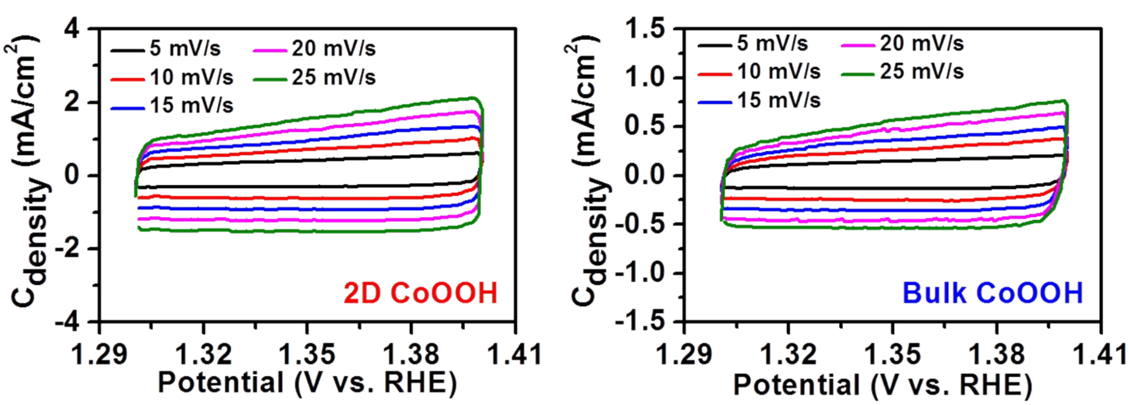

Figure S11. CV curves of 2D and bulk CoOOH at different scanning rates.

Table S2. Diffraction peaks of the XRD patterns.

	Bulk		nanosheets	
Materials	Location (2-Theta) (°)	Intensity (a.u.)	Location (2-Theta) (°)	Intensity (a.u.)
α-FeOOH	17.85	233	17.85	32
	21.25	1976	21.25	204
	26.35	169	26.35	34
	33.25	659	33.10	138
	34.70	40	34.60	54
	35.65	78	35.60	48
	36.10	271	36.05	64
	36.70	108	36.65	162
	39.10	58		
	40.20	58	40.15	44
	41.20	298	41.20	70
	43.25	32		
	53.30	61	53.20	70
	54.15	138	54.00	88
	55.30	50		
	57.50	36	57.45	32
	59.05	48	58.95	50
	61.50	68	61.25	40
	63.40	62		
	64.00	44	64.00	60
	65.70	14	65.70	22
	67.10	62		
	69.25	56	68.95	36
	71.85	36		
PbS	25.95	1658	25.95	335
	30.10	22467	30.10	517
	43.05	1530	43.00	265
	51.00	893	50.95	188
	53.45	298	53.40	107
	62.55	1860	62.55	69
	68.95	206	68.80	55
	70.95	531	70.90	108
	78.95	226	78.85	53
$CaCO_3$	23.05	175	23.05	38
	29.40	13639	29.40	536
	31.45	106	31.45	18
	35.95	283	35.95	68
	39.40	444	39.40	81
	43.15	428	43.15	101
	47.10	124	46.95	25

	47.55	747	47.55	93
	48.50	601	48.50	111
	56.60	101	56.55	19
	57.40	179	57.40	56
	58.10	41		
	60.70	101		
	61.05	452	61	27
	63.10	47		
	64.70	108	64.70	32
	65.65	130	65.65	27
	69.25	45		
	70.25	56		
	72.90	65	72.90	18
	73.70	28		
	76.30	39		
	77.20	75		

Table S3. Summarization of cleavage plane and 2D exfoliation of different non-layered materials. The non-layered materials that have been exfoliated to 2D materials are highlighted in green, and the non-layered materials that should be exfoliated to access 2D materials are highlighted in yellow.

Formula	Mineral material	Cleavage plane			
α-FeOOH	Goethite	(010)	(100)		
CoOOH	Heterogenite	(0001)			
TiO_2	Rutile	(110)	(100)	(111)	
Fe_3O_4	Magnetite	(111)			
PbS	Galena	(001)	(111)		
ZnS	Sphalerite	(011)			
NiS	Millerite	(10$\bar{1}$1)	(01$\bar{1}$2)		
CuS	Covellite	(0001)			
$CaCO_3$	Calcite	(10$\bar{1}$4)	(10$\bar{1}$0)	(11$\bar{2}$0)	(10$\bar{1}$1)
$ZnCO_3$	Smithsonite	(10$\bar{1}$1)			
$MnCO_3$	Rhodochrosite	(10$\bar{1}$1)	(10$\bar{1}$2)		
$FeCO_3$	Siderite	(10$\bar{1}$1)			
$PbCO_3$	Cerussite	(110)	(021)	(010)	(012)
$Cu_2CO_3(OH)_2$	Malachite	($\bar{2}$01)	(010)		
Al_2O_3	Corundum	(0001)	(10$\bar{1}$1)		

AlOOH	Diaspore	(010)	(110)	(100)	
AlOOH	Boehmite	(010)			
TiO_2	Anatase	(001)	(011)		
MnO_2	Pyrolusite	(110)			
SnO_2	Cassiterite	(100)	(110)	(111)	(011)
Cu_2O	Cuprite	(111)	(001)		
Cu_2S	Chalcocite	(110)			
FeS_2	Pyrite	(001)	(011)	(111)	
CdS	Greenockite	$(11\bar{2}2)$	(0001)		
$Ce(CO_3)F$	Bastnasite	$(10\bar{1}0)$	(0001)		
BiOCl	Bismoclite	(001)			

Table S4. Summarization non-layered materials that are considered non-exfoliatable to 2D materials (highlighted in red).

Formula	Mineral material	Cleavage plane
SiO_2	Quartz	No Cleavage
CuO	Tenorite	No Cleavage
Tl_2O_3	Avicennite	No Cleavage
Sb_2O_4	Clinocervantite	No Cleavage
Cr_2O_3	Eskolaite	No Cleavage
Ta_2O_5	Tantite	No Cleavage
$WO_3 \cdot 2H_2O$	Meymacite	No Cleavage
$WO_3 \cdot 0.5H_2O$	Elsmoreite	No Cleavage
$Sb_3O_6(OH)$	Stibiconite	No Cleavage
Cu_7S_4	Anilite	No Cleavage
Ni_3S_2	Heazlewoodite	No Cleavage
HgS	Hypercinnabar	No Cleavage
Sb_2S_3	Metastibnite	No Cleavage
$Rh_{17}S_{15}$	Miassite	No Cleavage
$AgBiS_2$	Schapbachite	No Cleavage
$FeSe_2$	Dzharkenite	No Cleavage

Ag_4SeS	Aguilarite	No Cleavage
$AgBiS_2$	Matildite	No Cleavage
$Cu_{31}S_{16}$	Djurleite	No Cleavage
$AgFe_2S_3$	Argentopyrite	No Cleavage
$TlFeS_2$	Raguinite	No Cleavage
$AlTaO_4$	Alumotantite	No Cleavage
$CuTeO_3$	Balyakinite	No Cleavage
$AlPO_4$	Berlinite	No Cleavage
$Fe(OH)_3$	Bernalite	No Cleavage
$AgBr$	Bromargyrite	No Cleavage
$AgCl$	Chlorargyrite	No Cleavage
$HgTe$	Coloradoite	No Cleavage
Cu_3As	Domeykite	No Cleavage
$Ca_3Si_2O_7$	Rankinite	No Cleavage
$ZrSiO_4$	Reidite	No Cleavage
Cu_7Te_5	Rickardite	No Cleavage
$FePO_4$	Rodolicoite	No Cleavage